

Article

Generalized Additive Model Reveals Nonlinear Trade-Offs/Synergies between Relationships of Ecosystem Services for Mountainous Areas of Southwest China

Qi Huang ^{1,2} , Li Peng ^{1,2,*} , Kexin Huang ^{1,2}, Wei Deng ^{1,2} and Ying Liu ^{1,2} 

- ¹ College of Geography and Resources, Sichuan Normal University, Chengdu 610101, China; 20211101021@stu.sicnu.edu.cn (Q.H.); 20201103003@stu.sicnu.edu.cn (K.H.); dengwei@imde.ac.cn (W.D.); liuying@imde.ac.cn (Y.L.)
- ² Key Laboratory of Land Resources Evaluation and Monitoring in Southwest, Ministry of Education, Sichuan Normal University, Chengdu 610101, China
- * Correspondence: pengli@imde.ac.cn

Abstract: Ecosystem services (ESs) are an essential link between ecosystems and human well-being, and trade-offs/synergies happen in ESs at different temporal and spatial scales. It is crucial to explore patterns of trade-offs/synergies among ESs, and their nonlinear relationships with changes in ESs. The primary objective of this study was to evaluate five ESs in 2000 and 2018: namely, water yield, food production, carbon sequestration, soil conservation, and habitat quality in mountainous regions of Southwest China. The mean values of the five ESs increased by 365.8 m³/ha, 13.92 t/hm², 497.09 TgC/yr², 138.48 t/km², and 0.002, respectively. Using spatial statistics and analysis, an ES trade-off synergy model (ESTD) was constructed for the five ESs change values. Overall, soil conservation has a trade-off with all five ESs, except habitat quality; this trade-off is increasing slightly. Water yield is in synergy with all ESs except soil conservation, with decreasing synergy; habitat quality is in synergy with all ESs except food production, with increasing synergy. Finally, the nonlinear relationship between the value of the change in the ES and ESTD was analyzed using a generalized additive model. Changes in water yield showed the greatest impact on ESTD except for food production, wherein changes in all three ESs had minimal impacts on ESTD. Food production dominates its trade-offs/synergies relationship with soil conservation; carbon sequestration is the dominant player in its trade-offs/synergies relationship with soil conservation. Habitat quality has a secondary position of influence, except in the trade-offs/synergies involving food production. By exploring the drivers of trade-offs/synergies among ESs, this study can provide guidance for the effective implementation of policies related to ecological protection and restoration.



Citation: Huang, Q.; Peng, L.; Huang, K.; Deng, W.; Liu, Y. Generalized Additive Model Reveals Nonlinear Trade-Offs/Synergies between Relationships of Ecosystem Services for Mountainous Areas of Southwest China. *Remote Sens.* **2022**, *14*, 2733. <https://doi.org/10.3390/rs14122733>

Academic Editors: Jeroen Meersmans and Yi Wang

Received: 24 April 2022

Accepted: 5 June 2022

Published: 7 June 2022

Publisher's Note: MDPI stays neutral with regard to jurisdictional claims in published maps and institutional affiliations.



Copyright: © 2022 by the authors. Licensee MDPI, Basel, Switzerland. This article is an open access article distributed under the terms and conditions of the Creative Commons Attribution (CC BY) license (<https://creativecommons.org/licenses/by/4.0/>).

Keywords: ecosystem service (ES); trade-offs/synergies; generalized additive model (GAM); Southwest China

1. Introduction

Ecosystem services (ESs) refer to the benefits that humans derive from ecosystems, integrating society and ecosystems to support the continued survival and development of human populations [1]. There are several types of ESs, each with drastically variable spatial distributions [2]. Large-scale ecological restoration projects are one of the key drivers of change in the relationships among various ESs [3]. These projects serve as good indicators for evaluating the ecological benefits of developmental projects by effectively linking human well-being to their surrounding environment [4]. In general, ES trade-offs involve an increase in one ES accompanied by a decrease in another ES [5]; synergy, on the other hand, refers to the simultaneous increase or decrease in ESs [6]. Consequently, understanding the factors that influence ES trade-offs is essential to maintaining a diverse and sustainable supply [7]. Trade-offs/synergies happen in ecosystems at different temporal and spatial scales,

and analyzing ESs dynamics is critical to understanding their trade-offs and synergies; ESs impact one another and can have some nonlinear responses [8]. Improving the current understanding of these linear or nonlinear relationships between ESs and quantitative expressions is a prerequisite for a thorough scientific assessment of ESs. Although remote sensing techniques are currently the most popular methods used to evaluate ESs, the quantitative and spatial response relationships between ESs trade-offs/synergies and ES changes need further clarification [9]. Previous research in this area focused on simple trade-offs and synergistic relationships among ecosystem services but neglected the exploration of the drivers and mechanisms of these relationships [10]. Although both external and internal factors influence relationships between ESs, trade-offs and synergistic relationships are of greater interest in response to ever-changing ESs. The generalized additive model [11] (GAM) is a semiparametric extension of the generalized linear model, which is a free and flexible statistical model that can handle nonlinear relationships between response variables and multiple explanatory variables using nonparametric smoothing functions [12]. It is not limited by the linear combination of explanatory variables and allows for the summation of various functions of explanatory variables. In addition, GAM is suitable for a variety of distribution types (e.g., Gaussian, binomial, gamma, and Poisson). Due to their various advantages, GAMs have been widely used in ecological and environmental health assessments in recent years. For example, Pu et al. [13] used a GAM to analyze the nonlinear relationship between socioeconomic circumstances and air pollution, and its effect on human life expectancy. Wahiduzzaman et al. [14] used a GAM and machine learning to model the effect of tropical cyclone activity on the northern Indian Ocean with the Boreal summer intra seasonal oscillation (BSISO) of the northern summer intra-seasonal oscillation.

GAMs have been used in relatively few investigations into ES trade-offs/synergies relationships, and our research used this model to analyze ES response relationships in Southwest China. This area is dominated by mountainous landscapes and is one of the most important regions for the function of ESs in China. The vegetation in Southwest China has improved in recent years [15]; changes in land-use types through ecological restoration projects have been considered to be the driving force behind this vegetation improvement phenomenon in Southwest China [16]. Coupled with accelerated urbanization and rapid climate change, there is immense pressure for urgent ecological conservation. Therefore, evaluating ESs and investigating the trade-offs/synergies relationship (and their drivers) between ESs has become an important theme in ecological management.

The state of ESs and their trade-off patterns are very complex due to the large internal variation and high substratum heterogeneity. Remote sensing data provide a relatively fast and convenient means to describe ESs' surface structures and functions at different temporal and spatial scales [17]. Moreover, remote sensing has tremendous advantages when monitoring ecological environment. The impact of changes in ESs on the trade-offs/synergies patterns is driven by both human activities and natural factors, and has not been well studied. In this study, we used remote sensing data and statistical data to conduct a study based on raster cells, which consisted of three main parts: (1) ES evaluation, (2) calculation of trade-offs/synergies, and (3) fitting response curves among ESs.

2. Materials and Methods

2.1. Study Area

Four provinces in Southwest China were studied, namely, Sichuan, Chongqing, Guizhou, and Yunnan, ranging from roughly 21° to 35°N (see Figure 1). The landscape of Southwest China is dominated by mountains and hills, making the local topography complex and diverse. This area is influenced by the East Asian monsoon and the South Asian tropical monsoon, resulting in a wide variety of climates and high diversity of vegetation types and ecosystems. Southwest China is rich in natural resources and is an important part of China's ecological security because of its high biodiversity and density of nature reserves, giving it the strategic function of providing ESs for all of China. Southwestern China contains the Karst Mountain range, one of the largest mountain regions in the world,

which is covered with exposed carbonate rocks. This is the distribution area of important ecological restoration projects by the Chinese government, such as returning farmland to forest and grass, and natural forest protection.

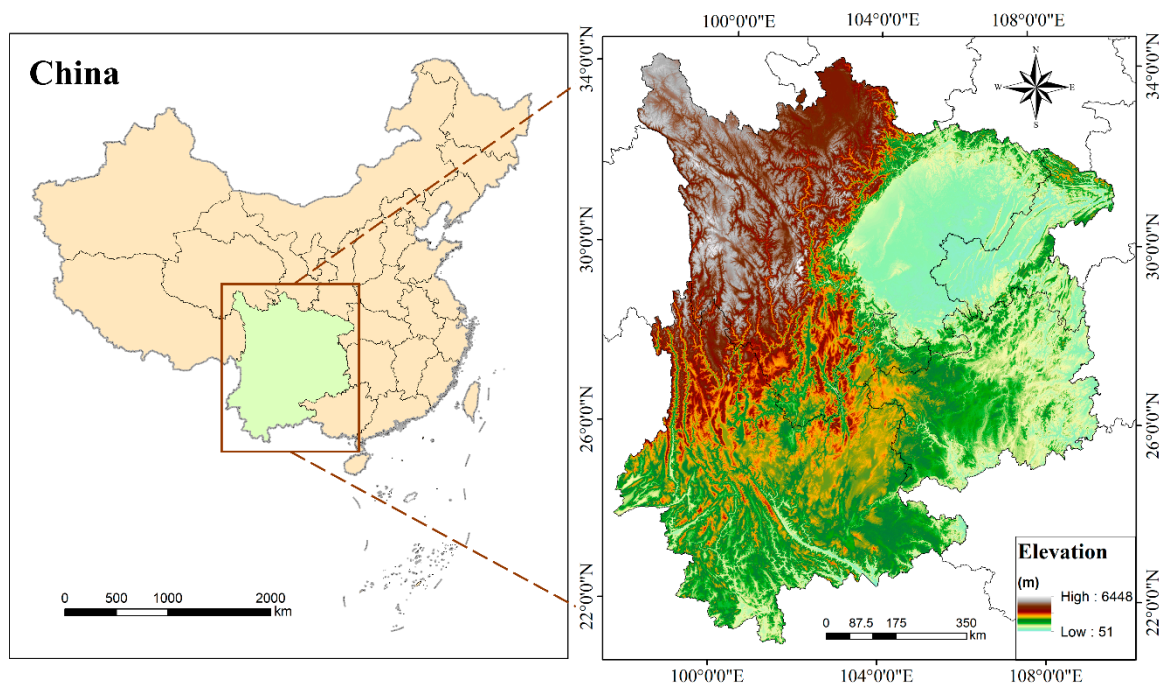


Figure 1. Location of study area.

2.2. Sources of Data

The data required for this study were: administrative boundaries from the National Bureau of Mapping and Geographic Information (<https://zwfw.ch.mnr.gov.cn/index>, accessed on 12 April 2022); land use type maps with land use data for 2000 and 2018 from the Earth System Science Data Sharing Platform (<http://www.geodata.cn/data/>, accessed on 12 April 2022); soil data focused on soil organic carbon content, soil capacity, and soil layer thickness from the China Soil Dataset, based on the World Soil Database (HWSD) (<http://data.tpd.ac.cn>, accessed on 12 April 2022); elevation data using the SRTMDEM-V2 product (<https://earthexplorer.usgs.gov/>, accessed on 12 April 2022) with a spatial resolution of 30 m; primary productivity (GPP) data from Data Publisher for Earth & Environmental Science (<https://www.pangaea.de/?t=Ecology>, accessed on 12 April 2022); biomass data from the Intergovernmental Panel on Climate Change (IPCC) (<https://www.ipcc.ch/data/>, accessed on 12 April 2022); and socioeconomic data from the Statistical Yearbook.

2.3. Methodology

The research framework consists of three major sections. With the combination of remote sensing data and statistical data, five ESs, i.e., water yield, food production, carbon sequestration, soil conservation, and habitat quality, were evaluated using spatial statistics and analysis methods; ESTD was used to investigate the trade-offs/synergies relationship between ESs. The nonlinear relationship between the changes in ES values and ESTD was analyzed using the GAM (see Figure 2).

2.3.1. ES Evaluation

Using remote sensing and statistical data, the InVEST model and ArcGIS 10.6 software were used to quantitatively assess five ecosystem services: water yield [18], carbon sequestration [19,20], soil conservation [21], habitat quality [22], and food production [23,24] in southwestern China and reveal their spatial and temporal patterns. The spatial resolution was treated as 1 km × 1 km, and calculations for the same are shown in Table 1.

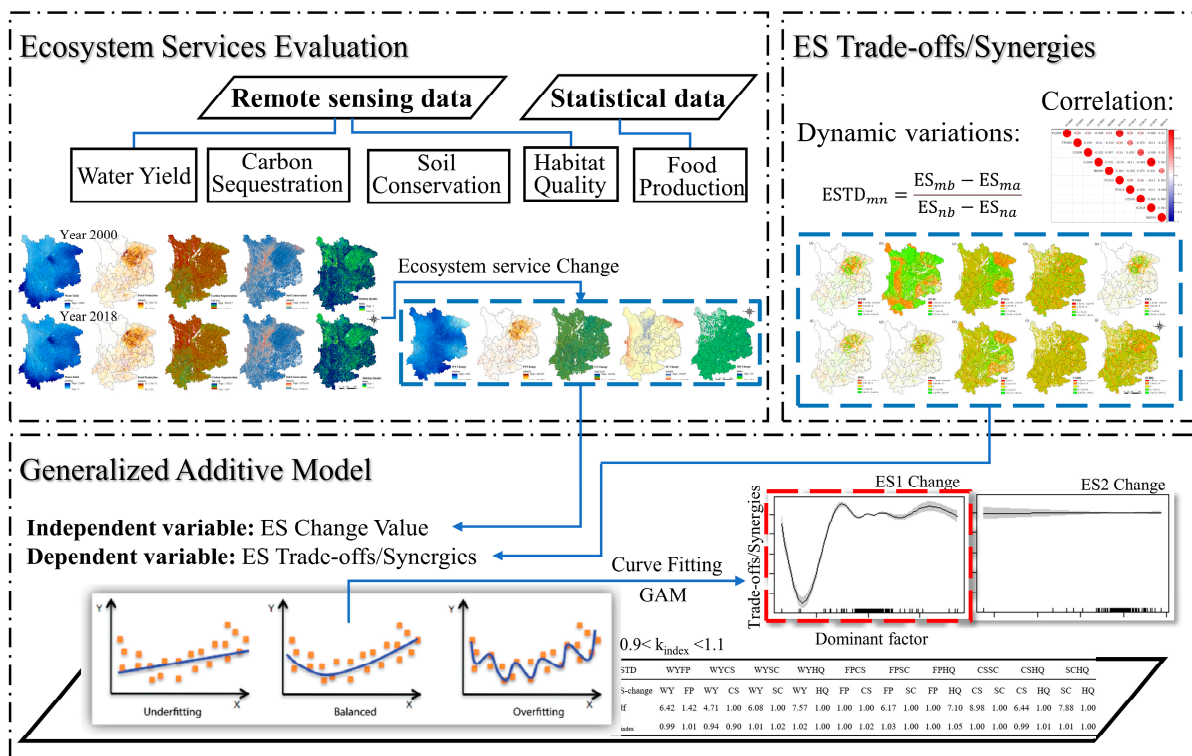


Figure 2. Framework of methodology.

Table 1. Calculation of ecosystem services.

ES	Calculation or Formula Model	Parameters and Processing
Water Yield	$Y(x) = P(x) - AET(x)$	$Y(x)$ is the average annual water yield, $P(x)$ is the average annual precipitation, and AET is actual evapotranspiration.
Carbon Sequestration	$GPP = PAR \times FPAR \times \epsilon_{max} \times \frac{1.1814 \times (1 + e^{0.3 \times (-T_{opt} - 10 + T_{air})})}{1 + e^{0.2 \times (T_{opt} - 10 - T_{air})}} \times (0.25 + 0.75 \times \frac{ET}{RN})$	PAR is calculated by multiplying CERES solar radiation and the monthly PAR/SW ratio derived from the BESS data set. ϵ_{max} and T_{opt} (i.e., maximum LUE and optimum growth temperature) refer to various flux measurements and sun-induced chlorophyll fluorescence values [19,20].
Soil Conservation	The Sediment Delivery Ratio model $RKLS = R \times K \times LS$ $USLE = R \times K \times LS \times C \times P$ $SD = RKLS - USLE$	$RKLS$ is the potential soil erosion (t) in the study area under specific landscape and climate conditions, $USLE$ is the actual amount of soil erosion (t) after taking into account the interception effect of vegetation and the implementation of management engineering measures, SD is soil retention (t), R is rainfall erosion force, K is soil erodibility, LS is the slope length slope factor, C is the vegetation cover factor, and P is the soil conservation measure factor.
Habitat Quality	The Habitat Quality model $Q_{xj} = H_j \left[1 - \left(\frac{D_{xj}^z}{D_{xj}^z + k^z} \right) \right]$	Q_{xj} is the habitat quality index of x grids in j habitats, H_j is the habitat suitability score of j habitats between 0 and 1, k is the half-saturation constant which is usually taken as 1/2 of the habitat degradation index, and z is the normalization constant, which is usually taken as the default value of 2.5.
Food Production	$G_i = \frac{G_{sum}}{NDVI_{sum}} \times NDVI_i$	G_i is the food production service of raster i , G_{sum} is the total food production of each county, $NDVI_{sum}$ is the sum of $NDVI$ of arable land-like elements in the county, and $NDVI_i$ is the $NDVI$ of raster i .

2.3.2. Trade-Off/Synergy Calculations

This study used the ecosystem services trade-off synergy model (ESTD) to evaluate the trade-offs/synergies relationships of the five ESs based on methods used in pre-existing studies [25]. It was used to assess the interactions and change mechanisms among ESs within the study area using the following equation:

$$\text{ESTD}_{mn} = \frac{\text{ES}_{mb} - \text{ES}_{ma}}{\text{ES}_{nb} - \text{ES}_{na}}, \quad (1)$$

where ESTD_{mn} is the degree of trade-off/synergy between the m th and n th ecosystem service, ES_{mb} is the change in the m th ES at time b , ES_{ma} is the change in the m th ES at time a , and ES_{nb} and ES_{na} are the same as above. $\text{ESTD} < 0$ indicates a trade-off between the m th and n th ESs, and $\text{ESTD} > 0$ indicates a synergistic relationship between the two.

2.3.3. Fitting the Response Curve among ESs

GAMs can be used to test for nonlinear relationships between variables when the relationship between explanatory and effect variables is uncertain. Many ecological data do not fit into simple linear models, and GAMs are data-driven nonparametric regression models that are nonparametric extensions of traditional generalized linear models. The connections between ecosystem processes, functions, and benefits to humans are complex and dynamic, suggesting that the relationships between these variables are often nonlinear [26]. GAMs do not require parametric models to be set up in advance, and unlike parametric multiple regressions, additive models relax restrictions on the additive form of response relationships; this allows arbitrary sums of functions to model the results, and relationships between independent and response variables can be arbitrarily linear or nonlinear.

The nonlinear relationship between ESTD and the value of each ES change was established based on a smooth function of each explanatory variable. The nonlinear model was constructed through the GAM function of the `mgcv` package [27] in R 4.1.1. The model can be written as the following equation:

$$g(y_i) = \beta_0 \sum_{i=1}^n s_i(x_i) + \varepsilon_i, \quad (2)$$

where y is ESTD, β_0 is the overall average value of the response variable, $s_i(x_i)$ is the smoothing function for the i th ES change value, n is the total number of covariables, and ε_i is the residual. The smoothing function is represented by model selection and automatic smoothing parameter selection for penalized regression splines, which optimizes the number of dimensions in the fitted and minimized model.

3. Results

3.1. ESs

The mean values of water yield, food production, carbon sequestration, soil conservation, and habitat quality all increased in the four provinces of Southwest China from 2000 to 2018, from 9083.4 m³/ha, 277.06 t/hm², 1510.97 TgC/yr², 52,094.39 t/km², and 0.834 in 2000 to 9449.2 m³/ha, 290.98 t/hm², 1649.45 TgC/yr², 52,591.48 t/km², and 0.836 in 2018, respectively; these represent increases of 365.8 m³/ha, 13.92 t/hm², 497.09 TgC/yr², 138.48 t/km², and 0.002, respectively.

Considering spatial distribution, in Figure 3, high values of water yield are mainly distributed towards the west of the Sichuan Basin, the north of Chongqing city, and the south of Yunnan and Guizhou; high values of food production are mainly in the Sichuan Basin, with little food production in the northwest Sichuan plateau. High values of carbon sequestration are more concentrated in the Yunnan province, while high values of soil conservation are mainly distributed in the west of Sichuan, the west of the Yunnan-Guizhou plateau, and the north of Chongqing; low values are mainly concentrated in the Chengdu plain. High values of habitat quality are distributed in areas outside the Sichuan Basin and the western Sichuan Plateau, at an altitude of 4000 m. Changes in the mean values of

ESs indicate that human activities and climate change have resulted in positive impacts; the implementation of national policies and ecological projects have resulted in positive impacts on the five ESs considered in this study.

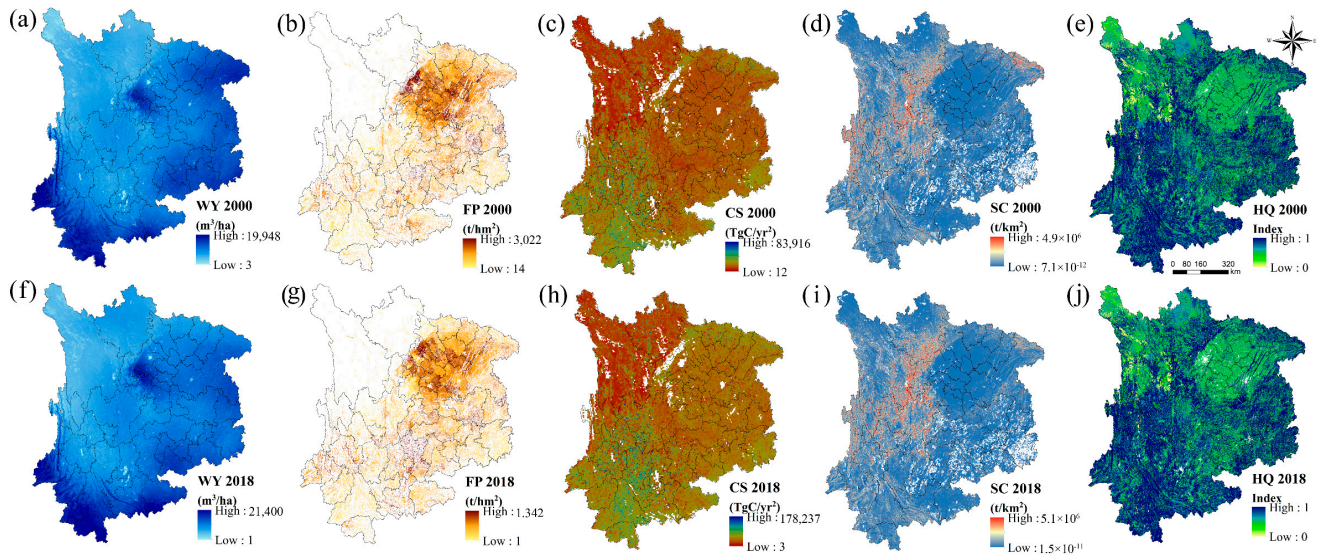


Figure 3. Spatial distribution of five ecosystem services in 2000 and 2018. WY: Water Yield; FP: Food Production; CS: Carbon Sequestration; SC: Soil Conservation; HQ: Habitat Quality. WY 2000 is the water yield in 2000. WY 2018 is the water yield in 2018. Same for the rest.

Although the overall average values of various ESs increased from 2000 to 2018, there were large spatial differences within them. In Figure 4a, WY had a relatively high increase in the southern, northern, and central regions of Southwest China, with a significant decrease in northern Chongqing; in Figure 4b, the elevated values in FP are mainly located in the Sichuan Basin. The distribution of regions with increased CS (Figure 4c) and significantly increased FP are relatively similar, and the decrease in SC is mainly located in western Yunnan Province and northern Chongqing (Figure 4d); the increase is mainly in central Sichuan. This pattern is consistent with the spatial variation of WY in Figure 4e, HQ is significantly improved in the southwest part of Chongqing and in western Sichuan.

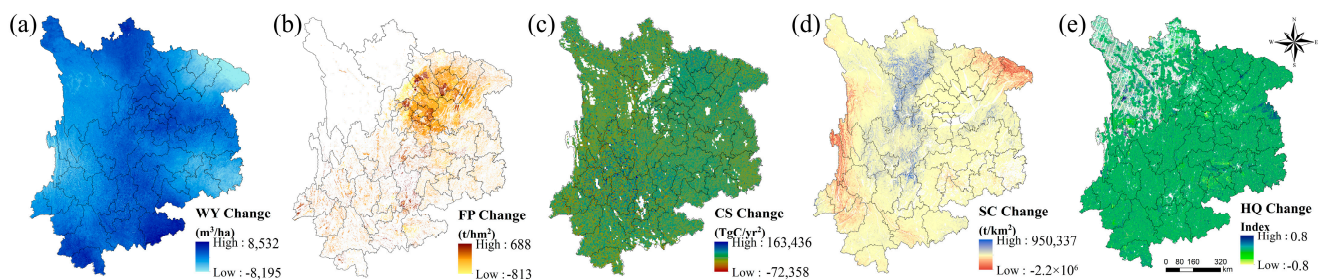


Figure 4. Spatial variations of five ecosystem services from 2000 to 2018. WY Change: the change in Water Yield from 2000 to 2018. FP Change: the change in Food Production. CS Change: the change in Carbon Sequestration. SC Change: the change in Soil Conservation from 2000–2018. HQ Change: the change in Habitat Quality.

3.2. ESs Trade-Off/Synergy

3.2.1. ESs Correlation

Correlation coefficients between the 2000 and 2018 ESs were plotted using correlation analysis, and all significance tests satisfied $p < 0.05$, except for the insignificant correlation between FP and HQ in 2018. In Figure 5, WY shows a synergistic relationship with all ESs except SC; SC has a trade-off between WY and FP. The synergy between WY and FP

increased from 2000 to 2018. There was a very weak and decreasing trade-off between SC and CS, while the relationship between SC and HQ was synergistic and increasing. FP was synergistically related to WY and CS, with a synergistic decrease in WY and an increase in CS. FP and HQ are trade-offs that have been increasing slightly. Excluding the increased trade-off between HQ and FP, HQ was in synergy with all other ESs. The synergy between SC and CS has been steadily increasing, and the synergy between SC and WY gradually decreased.

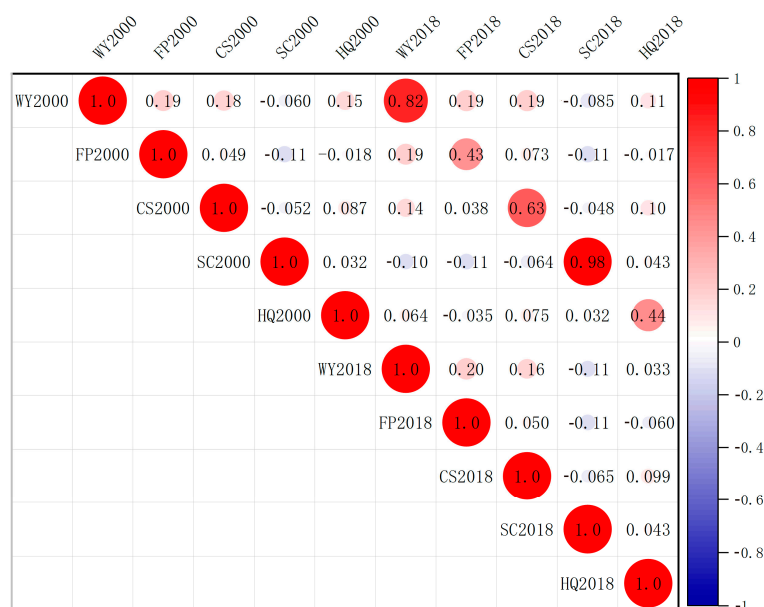


Figure 5. Correlations between category five ecosystem services in 2000 and 2018. WY2000: Water Yield in year 2000; WY2018: Water Yield in year 2018. Same for the rest.

SC generally showed a trade-off with all ESs except habitat quality, which had a slightly increasing trade-off. WY showed synergy with all ESs except SC; the synergy was decreasing. HQ showed synergy with all ESs except FP, wherein the synergy showed an increasing trend.

3.2.2. ESTD Results

The area and spatial distribution of ES changes were investigated using the dynamic change values [28] of each ES in 2000 and 2018 to calculate the ESTD of the five ES changes.

It can be seen that the high trade-off between WY and CS was mainly distributed in the northeastern and southeastern parts of the study area, while the synergy between WY and SC was as high as 69.35% of the total area; this is consistent with the distribution of change values in Table 2. The synergy between CS and SC was also relatively significant, accounting for 53.28% of the total area in Figure 6. The trade-off between FP and SC was relatively large, accounting for 47.92% of the total area; the trade-off between SC and HQ is also relatively significant. As a whole, the trade-off/synergy between WY and SC, WY and CS, and SC and CS are spatially clustered over a large area, while the trade-offs and synergies of the remaining ESs are more well-dispersed.

Table 2. The area of synergy of trade-offs between the value of change in ecosystem services. WY-FP is the ESTD of WY and FP. Same for the rest. ESTD < 0 indicates a trade-off between the two ESs and ESTD > 0 indicates a synergistic relationship.

	WY-FP	WY-CS	WY-SC	WY-HQ	FP-CS	FP-SC	FP-HQ	CS-SC	CS-HQ	SC-HQ
Trade-off	50.02%	45.23%	30.65%	51.05%	49.23%	52.08%	50.89%	46.72%	51.46%	51.86%
Synergy	49.98%	54.77%	69.35%	48.95%	50.77%	47.92%	49.11%	53.28%	48.54%	48.14%

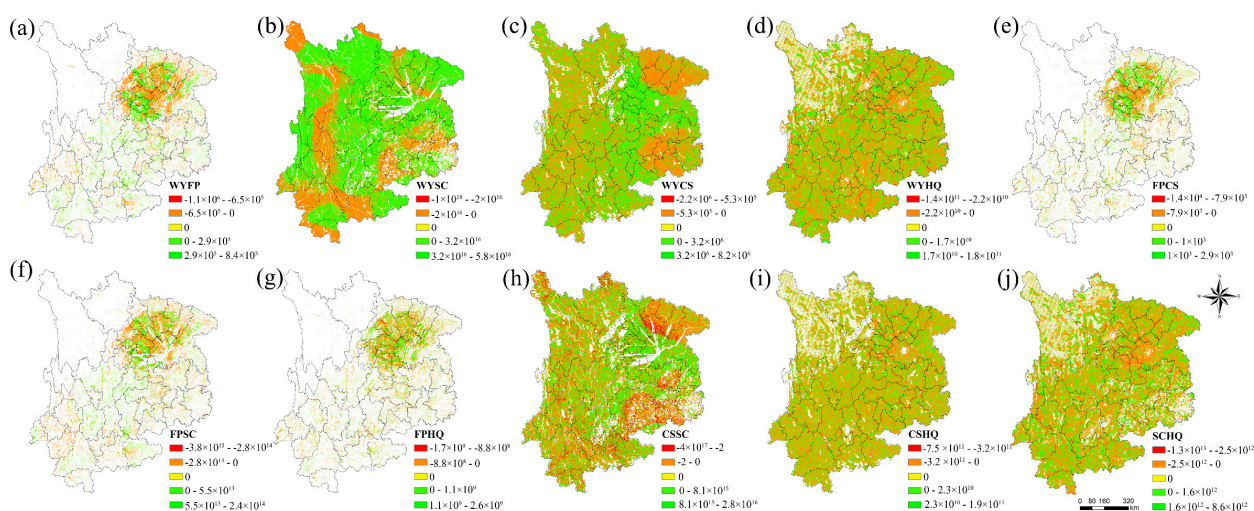


Figure 6. Spatial distribution of trade-offs/synergies for five ecosystem services. WYFP is the ESTD of WY and FP. WYSC is the ESTD of WY and SC. Same for the rest.

Figure 7 shows the distribution of ES change data in a reciprocal trade-off/synergistic relationship with the data normalized in advance. Each violin plot represents the data distribution; most data distributions are relatively concentrated, with discrete values for some FP and CS. Similar to the kernel density plot readings, the peak heights represent the probability density of the data, with higher peaks being denser. In Figure 7a, taking WY in WYFP as an example, it is obvious that the first orange box is wider at $y > 0$ than at $y < 0$, i.e., it indicates that most of the WY data are positive when WY presents a trade-off with FP. Another example is in Figure 7a,b, where SC in WYSC shows a different form of data distribution in a trade-off or synergistic relationship with WY. When synergistic relationships are present Figure 7b, SC data are more dispersed. In Figure 7a,b, the probability density of FP in FPSC in the trade-off/synergy relationship with SC is larger for $FP < 0$ data under the trade-off relationship than for $FP < 0$ data under the synergistic relationship.

3.3. Response Curves of ES Trade-Offs/Synergies

A nonlinear relationship between ES trade-offs/synergies and the change values of each ES was established based on a smooth function of each explanatory variable, where the horizontal coordinate is the value of change in ESs and the vertical coordinate is ESTD.

Analysis of the results in Figure 8a shows that the increase in negative variation of WY makes WY gradually converge with FP. Since the negative variation of WY tends from $-1300 \text{ m}^3/\text{ha}$ to $-3000 \text{ m}^3/\text{ha}$, WY and FP gradually convert from a synergy to a trade-off. The positive increase in WY makes it gradually tend to synergize with FP, shifting to a trade-off trend when the positive change is greater than $1800 \text{ m}^3/\text{ha}$. As FP increases, the trade-off with WY gradually increases; an increase in the negative change in FP tends to be synergistic.

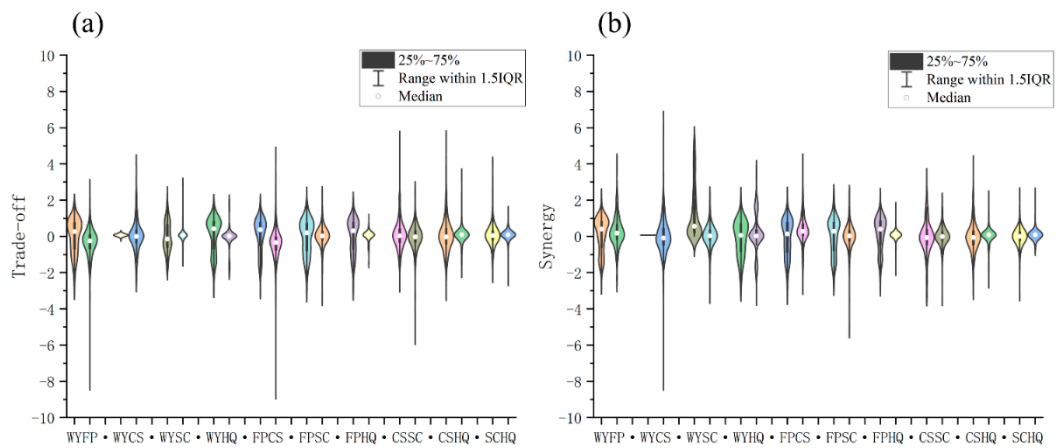


Figure 7. ES variation kernel density estimation map. (a) shows the kernel density estimates for the interaction trade-off relationship. (b) shows the kernel density estimates for the interaction synergy relationship. Here, white dots in the center of each violin shape represent the median of data, which can reflect the overall situation of the data. The length of the violin body indicates the degree of dispersion of the data, while the highest and lowest points of the body indicate 25% and 75% of the values, respectively. The top and bottom extend to a maximum of $1.5 \times$ IQR (interquartile range).

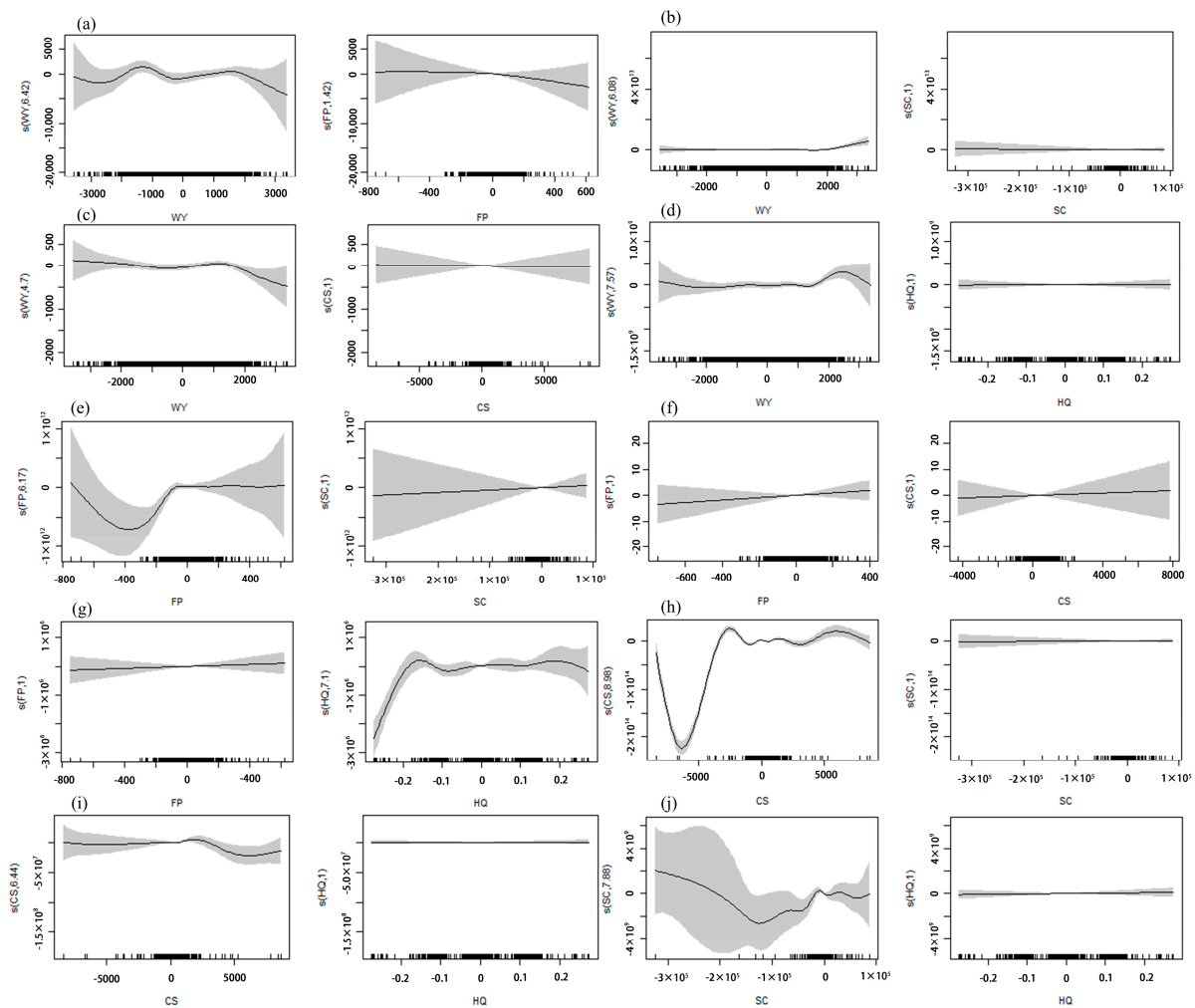


Figure 8. Relationship between trade-offs/synergies among ESs (a–j).

In Figure 8b, when the negative change in WY increases or the positive change is insignificant, the ESTD interaction remains relatively unchanged. As the positive change in

the WY increased to 1500 m³/ha, a synergistic effect with SC began to arise. Changes in SC had little effect on ESTD.

In Figure 8c, an increase in the negative change in WY promotes a synergistic relationship with CS. The increase in positive variation will lead to the generation of synergy before the appearance of a trade-off; the synergy peaks when increasing to 1500 m³/ha, after which a trade-off trend will appear. Changes in CS showed very little effect on their ESTD.

In Figure 8d, as the positive change in WY increases, the synergistic relationship with HQ becomes clearer; however, when increased to 2500 m³/ha, the synergy begins to decline. After 3500 m³/ha, the trade-off trend begins, and the increase in negative changes will have some synergistic effect. Changes in HQ showed very little effect on ESTD.

Figure 8a–d show that the effect of changes in the volume of WY dominated the ESTD with other ESs; except for FP, changes in all three ESs do not show a large impact on ESTD.

In Figure 8e, as the negative change in FP increases, a peak in the trade-off relationship with SC is reached around 400 t/hm², after which the trend becomes synergistic. Positive increases in SC show synergistic effects, and negative increases show trade-offs.

In Figure 8f, trends in FP are relatively similar to those in CS. An increase in positive changes produces a synergistic effect between them, and an increase in negative changes produces a trade-off trend.

In Figure 8g, a positive increase in FP shows synergies, and a negative increase appears as a trade-off trend. The trade-off increases gradually as the change in HQ increases from −0.17 to −0.2; the negative change from 0 to −0.17 produces a trend of trade-offs followed by synergies, with the dividing line at approximately −0.1. The value of positive changes in HQ (greater than 0.2) tends to be a trade-off from a synergy.

The synergy and trade-off trend between CS and SC in Figure 8h is similar to that between FP and SC in Figure 8e. An increase in positive or negative changes in CS causes it to maintain a synergy and then a trade-off with the SC. The trade-offs weaken and gradually converge to synergy as the negative change in CS increases above about −5000 TgC/yr². Changes in SC basically do not affect their ESTD.

In Figure 8i, the increase in the negative change in CS has little effect on ESTD. The increase in positive change causes the ESTD between CS and HQ to fluctuate: a synergy is created first, followed by trade-off increases. After about 5000 TgC/yr², the trade-off starts to decrease. The effect of changes in HQ on the trade-off synergy is negligible.

In Figure 8j, the trade-off effect diminishes as the negative change in SC increases, after increasing to -1.3×10^5 , t/km². At -2×10^5 , t/km², the trade-off tends to become a synergy, and the increase in positive change causes it to fluctuate around the trade-off synergy. Changes in HQ had little effect on ESTD.

Figure 8e–j show that FP dominates the ESTD between it and SC; CS is the dominant player between CS and SC; HQ occupies a secondary position of influence except in the trade-off synergy with FP.

The GAM fitting results for each ES change were evaluated through a smoothness test (see Table 3). When $kindex < 0.9$ or > 1.1 , the smoothing function adds degrees of freedom to improve the smoothness of the curve. “edf” is the degree of freedom and higher edf values indicate more complex spline curves. A degree of freedom larger than 1 indicates a curvilinear relationship. Theoretically, when the degree of freedom is close to 1, it indicates a linear relationship.

Table 3. Smoothness test for GAMs.

	WY-FP		WY-CS		WY-SC		WY-HQ		FP-CS		FP-SC		FP-HQ		CS-SC		CS-HQ		SC-HQ	
ES-change	WY	FP	WY	CS	WY	SC	WY	HQ	FP	CS	FP	SC	FP	HQ	CS	SC	CS	HQ	SC	HQ
edf	6.42	1.42	4.71	1.00	6.08	1.00	7.57	1.00	1.00	1.00	6.17	1.00	1.00	7.10	8.98	1.00	6.44	1.00	7.88	1.00
Kindex	0.99	1.01	0.94	0.90	1.01	1.02	1.02	1.00	1.00	1.02	1.03	1.00	1.00	1.05	1.00	1.00	0.99	1.01	1.01	1.00

4. Discussion

4.1. ES Assessment

Under natural and human-induced influences, the five ESs (water yield, food production, carbon sequestration, soil conservation, and habitat quality) in the mountainous regions of Southwest China show an increasing trend, which is inextricably linked to the implementation of ecological protection policies. This is consistent with previous studies in Southwest China, with slight differences in research methodology, time scales, and spatial scales. The Chinese government launched the “Natural Forest Protection Project” in 1998 and the “Regional Effects of Grain for Green Program” in 2000 to promote the reforestation of mountainous areas; these are the largest ecological restoration projects in the world, in terms of scale and financial investment. These projects have covered 44.8% of China’s forests and 23.2% of China’s grasslands. These projects have produced many achievements, including substantial increases in vegetation cover [29,30], improved biodiversity [31], and reduced erosion [32] and flood [33] risks; these positive impacts have had a positive effect on ESs. In recent years, China has undergone rapid urbanization and national key restoration projects, and the promotion of mountain reforestation has brought about large-scale vegetation restoration. Most scholars focus on the domestic policy outcome-oriented perspective for large-scale ES studies, in fact, ES can also be explored from the perspective of human perception in conjunction with population or cities. For example, some very interesting international research has also been conducted. Battisti et al. explored the user perception of aesthetic quality under different landscape elements based on a participatory approach [34]. Another study identified specific sites that could be improved to enhance ESs by combining with socio-demographic factors [35]. An assessment of ecosystem services in the Oslomarka forest was conducted in the context of the growing academic interest in urban and peri-urban forests [36].

4.2. ES Trade-Offs/Synergies

In the study of tradeoffs/synergies among ESs, many quantitative methods have been used to quantify and analyze ESs trade-offs/synergies, including correlation analysis [37,38], cluster analysis [3], redundancy analysis (RDA) [39], and multivariate regression trees [40]. Studies on trade-offs/synergies in ESTD consider the ecosystem services at two time points. Current research in this approach has made some progress [41]. Although many studies have been carried out to investigate the trade-offs/synergies relationships and their spatiotemporal variations, the factors underlying these complex interactions are still poorly understood [25]. It is essential to reveal the trade-offs/synergies and the spatial differences in the services. Understanding the trade-offs/synergies among ESs is insufficient without carefully exploring the drivers and mechanisms behind the relationships [42]. The formation of tradeoffs and synergies among ecosystem services can be attributed to one or more of the following three factors: land use conflict or consistency, common drivers, and interactions among ecosystem services [43]. The spatial variation of land use/cover caused by human activities is an important factor affecting the degree of ES tradeoffs and its scale effect [44].

4.3. GAM Response Curves

Based on the study of simple trade-off/synergistic relationships among ESs, the drivers of these relationships were further explored. Yang et al. [45] compared ESs in the lower reaches of the Pearl River at different levels of urbanization; Peng et al. [46] researched the relationship between ESs and urbanization in the mountainous regions of southwest China; Luo et al. [47] analyzed the impact of land use change on the trade-offs of ESs in the Chishui River basin; Chen et al. [48] explored the human- and climate-driven mechanisms of changes in trade-offs between ESs in the Chengdu-Chongqing urban agglomeration, and the influence of national policies; and Qiu et al. [49] analyzed the effects of topographic factors, soil texture, and human activities on trade-offs of ESs in different climatic zones in Shaanxi Province. This study used a GAM to establish a nonlinear relationship between ESTD and the changing values of each ES, based on a smooth function of each

explanatory variable. By plotting response curves, we can identify the dominant services in the trade-off/synergistic relationship between ESs, which assists the macro-regulation of ESs. We found that WY dominated most of the trade-off/synergistic relationships, and the influence of FP was relatively large, with SC and HQ usually having a comparatively smaller influence. Such research provides important information for ecological conservation and restoration, thus helping understand human and natural impacts on ecosystems. For example, Figure 8a shows that the trade-off/synergy relationship between WY and FP gradually decreases from higher synergy when WY changes up to a certain level. As WY increases, the synergistic relationship changes to a trade-off relationship. Such regularity provides a quantitative reference for the agricultural rationalization of irrigation and drainage, providing inspiration for the change in trade-off/synergy between ESs.

Watson [50] explained that rapid changes in potential drivers or interactions among drivers may lead to abrupt ecosystem changes without positive feedback mechanisms. The nonparametric smoothing approach of the GAM describes some of the potential nonlinear response patterns that are not captured by linear models, such as fluctuating increases or decreases. Such fluctuations, however, are very likely due to data instability, higher dispersion, or random errors, potentially introducing misunderstandings in the interpretation of the synergistic response implications of ES trade-offs. Regardless of this, additive models have high application value and can be used as exploratory tools. Many scholars have improved upon this model, e.g., Xue and Liang [51] studied a semiparametric generalized additive model (GACM) that generalizes the prediction function in a conventional GAM to an unknown function that depends on some covariates to overcome the “curse of dimensionality” problem when the tuning variables are large. Wood et al. [52] proposed a method for efficient selection of model smoothness for GAM, which yields reliable results by optimizing the entire model; the authors also investigated a GAM model for large data sets [53].

Figure 8 shows that there are some response curves fitted using the GAM for which the results are already close to a linear relationship (i.e., edf = 1); results are still linear when the number of basic smoothing functions is further adjusted using the guarantee of smoothness test. The linearity result proves that there is no overfitting problem and highlights the dominance of nonlinear ES variation in ESTD. Thus, the use of a GAM in the search for the dominant influence amongst various ESs’ trade-offs/synergies can still be relatively obvious. This facilitates further conclusions and lays the foundation for future research.

5. Conclusions

Using Southwest China as the study area, this study assessed five ESs in 2000 and 2018 using remote sensing and statistical yearbook data; their distributions were then discussed. Based on this analysis, the trade-off/synergistic relationships of the five changing ES values were analyzed using spatial statistics and analysis methods. The generalized additive model (GAM) was then used to analyze the nonlinear relationship between the change values of ESs and ESTD in order to understand the patterns of change in various types of ESs that affect the trade-off/synergistic relationships among ESs. The main conclusions are as follows. The mean values of five ESs—water yield, food production, carbon sequestration, soil conservation, and habitat quality—all increased in four provinces of Southwest China from 2000 to 2018, increasing by 365.8 m³/ha, 13.92 t/hm², 497.09 TgC/yr², 138.48 t/km², and 0.002, respectively. Calculation of ESTD for the five ESs revealed that: soil conservation is traded off with all ESs except habitat quality, and this trade-off increases slightly; water yield is in synergy with all ESs except soil conservation, with synergy decreasing; and habitat quality is in synergy with all ESs except food production, wherein synergy tends to increase. Finally, the nonlinear relationship between the value of the change in ESs and ESTD was analyzed using GAMs. Changes in water yield had the greatest impact on ESTD compared to other ESs, except food production, wherein changes in all three ESs did not have a large impact on ESTD. Food production dominates the trade-offs/synergies relationship between it and soil conservation, and in carbon sequestration and soil conservation;

carbon sequestration is the dominant player in their trade-offs/synergistic relationship. Habitat quality occupies a secondary position of influence, except in trade-offs/synergies involving food production. Due to the huge internal variation in different study areas and high substratum heterogeneity, the trade-offs/synergies of ESs present a complex nonlinear relationship. The flexibility of GAMs enables the mapping of the response curve between the ESs and trade-offs/synergies, which is applicable to the exploration of the driving factors.

Author Contributions: Q.H.: methodology, software, validation, formal analysis, writing—original draft. L.P.: methodology, investigation, resources, data curation, supervision. K.H.: data curation, methodology, visualization. W.D.: resources, supervision. Y.L.: investigation, data curation. All authors have read and agreed to the published version of the manuscript.

Funding: This work is funded by the National Natural Science Foundation of China (42071222), the Sichuan Science and Technology Program (2022JDJQ0015), and the Tianfu Qingcheng Program (ZX20220027).

Data Availability Statement: Data are not currently available to the public as of the publication of this paper.

Conflicts of Interest: The authors declare that they have no known competing financial interest or personal relationship that could have appeared to influence the work reported in this paper.

References

- Douglas, I. Ecosystems and Human Well-Being. In *Reference Module in Earth Systems and Environmental Sciences*; Elsevier: Amsterdam, The Netherlands, 2015; p. B978012409548909206X. ISBN 978-0-12-409548-9.
- Fisher, B.; Turner, R.K.; Morling, P. Defining and Classifying Ecosystem Services for Decision Making. *Ecol. Econ.* **2009**, *68*, 643–653. [CrossRef]
- Chen, H.; Fleskens, L.; Schild, J.; Moolenaar, S.; Wang, F.; Ritsema, C. Using Ecosystem Service Bundles to Evaluate Spatial and Temporal Impacts of Large-Scale Landscape Restoration on Ecosystem Services on the Chinese Loess Plateau. 2021. Available online: <https://www.researchsquare.com/article/rs-273669/v1.pdf> (accessed on 23 April 2022).
- Gao, J. Editorial for the Special Issue “Ecosystem Services with Remote Sensing”. *Remote Sens.* **2020**, *12*, 2191. [CrossRef]
- Felipe-Lucia, M.R.; Comín, F.A.; Bennett, E.M. Interactions Among Ecosystem Services Across Land Uses in a Floodplain Agroecosystem. *Ecol. Soc.* **2014**, *19*, art20. [CrossRef]
- Bennett, E.M.; Peterson, G.D.; Gordon, L.J. Understanding Relationships among Multiple Ecosystem Services: Relationships among Multiple Ecosystem Services. *Ecol. Lett.* **2009**, *12*, 1394–1404. [CrossRef]
- Qian, D.; Du, Y.; Li, Q.; Guo, X.; Cao, G. Alpine Grassland Management Based on Ecosystem Service Relationships on the Southern Slopes of the Qilian Mountains, China. *J. Environ. Manag.* **2021**, *288*, 112447. [CrossRef] [PubMed]
- Shen, J.; Li, S.; Liang, Z.; Liu, L.; Li, D.; Wu, S. Exploring the Heterogeneity and Nonlinearity of Trade-Offs and Synergies among Ecosystem Services Bundles in the Beijing-Tianjin-Hebei Urban Agglomeration. *Ecosyst. Serv.* **2020**, *43*, 101103. [CrossRef]
- Cord, A.F.; Bartkowski, B.; Beckmann, M.; Dittrich, A.; Hermans-Neumann, K.; Kaim, A.; Lienhoop, N.; Locher-Krause, K.; Priess, J.; Schröter-Schlaack, C.; et al. Towards Systematic Analyses of Ecosystem Service Trade-Offs and Synergies: Main Concepts, Methods and the Road Ahead. *Ecosyst. Serv.* **2017**, *28*, 264–272. [CrossRef]
- Chen, H.; Fleskens, L.; Schild, J.; Moolenaar, S.; Wang, F.; Ritsema, C. Impacts of Large-Scale Landscape Restoration on Spatio-Temporal Dynamics of Ecosystem Services in the Chinese Loess Plateau. *Landsc. Ecol.* **2022**, *37*, 329–346. [CrossRef]
- Chiang, A.Y. Generalized Additive Models: An Introduction with R. *Technometrics* **2007**, *49*, 360–361. [CrossRef]
- Wang, F.; Yuan, X.; Zhou, L.; Liu, S.; Zhang, M.; Zhang, D. Detecting the Complex Relationships and Driving Mechanisms of Key Ecosystem Services in the Central Urban Area Chongqing Municipality, China. *Remote Sens.* **2021**, *13*, 4248. [CrossRef]
- Pu, H.; Wang, S.; Wang, Z.; Ran, Z.; Jiang, M. Non-Linear Relations between Life Expectancy, Socio-Economic, and Air Pollution Factors: A Global Assessment with Spatial Disparities. *Environ. Sci. Pollut. Res.* **2022**. [CrossRef]
- Wahiduzzaman, M.; Luo, J.-J. Modeling of Tropical Cyclone Activity over the North Indian Ocean Using Generalised Additive Model and Machine Learning Techniques: Role of Boreal Summer Intraseasonal Oscillation. *Nat. Hazards* **2022**, *111*, 1801–1811. [CrossRef]
- Mu, B.; Zhao, X.; Wu, D.; Wang, X.; Zhao, J.; Wang, H.; Zhou, Q.; Du, X.; Liu, N. Vegetation Cover Change and Its Attribution in China from 2001 to 2018. *Remote Sens.* **2021**, *13*, 496. [CrossRef]
- Tong, X.; Brandt, M.; Yue, Y.; Horion, S.; Wang, K.; Keersmaecker, W.D.; Tian, F.; Schurgers, G.; Xiao, X.; Luo, Y.; et al. Increased Vegetation Growth and Carbon Stock in China Karst via Ecological Engineering. *Nat. Sustain.* **2018**, *1*, 44–50. [CrossRef]
- Editorial Department of Journal of Remote Sensing. Briefing on “Remote Sensing Scale Effects and Scale Conversion” Forum. *J. Remote Sens.* **2014**, *18*, 735–740.

18. Ran, C.; Wang, S.; Bai, X.; Tan, Q.; Zhao, C.; Luo, X.; Chen, H.; Xi, H. Trade-Offs and Synergies of Ecosystem Services in Southwestern China. *Environ. Eng. Sci.* **2020**, *37*, 669–678. [[CrossRef](#)]
19. Chen, Y.; Feng, X.; Fu, B.; Wu, X.; Gao, Z. Improved Global Maps of the Optimum Growth Temperature, Maximum Light Use Efficiency, and Gross Primary Production for Vegetation. *J. Geophys. Res. Biogeosci.* **2021**, *126*, e2020JG005651. [[CrossRef](#)]
20. Chen, Y.; Feng, X.; Tian, H.; Wu, X.; Gao, Z.; Feng, Y.; Piao, S.; Lv, N.; Pan, N.; Fu, B. Accelerated Increase in Vegetation Carbon Sequestration in China after 2010: A Turning Point Resulting from Climate and Human Interaction. *Glob. Chang. Biol.* **2021**, *27*, 5848–5864. [[CrossRef](#)]
21. Tesfaye, A.; Brouwer, R. Testing Participation Constraints in Contract Design for Sustainable Soil Conservation in Ethiopia. *Ecol. Econ.* **2012**, *73*, 168–178. [[CrossRef](#)]
22. Wang, B.; Cheng, W. Effects of Land Use/Cover on Regional Habitat Quality under Different Geomorphic Types Based on InVEST Model. *Remote Sens.* **2022**, *14*, 1279. [[CrossRef](#)]
23. Smith, P. Delivering Food Security without Increasing Pressure on Land. *Glob. Food Secur.* **2013**, *2*, 18–23. [[CrossRef](#)]
24. Zhang, T.; Zhang, S.; Cao, Q.; Wang, H.; Li, Y. The Spatiotemporal Dynamics of Ecosystem Services Bundles and the Social-Economic-Ecological Drivers in the Yellow River Delta Region. *Ecol. Indic.* **2022**, *135*, 108573. [[CrossRef](#)]
25. Li, M.; Zheng, P.; Pan, W. Spatial-Temporal Variation and Tradeoffs/Synergies Analysis on Multiple Ecosystem Services: A Case Study in Fujian. *Sustainability* **2022**, *14*, 3086. [[CrossRef](#)]
26. Costanza, R.; de Groot, R.; Braat, L.; Kubiszewski, I.; Fioramonti, L.; Sutton, P.; Farber, S.; Grasso, M. Twenty Years of Ecosystem Services: How Far Have We Come and How Far Do We Still Need to Go? *Ecosyst. Serv.* **2017**, *28*, 1–16. [[CrossRef](#)]
27. Pedersen, E.J.; Miller, D.L.; Simpson, G.L.; Ross, N. Hierarchical Generalized Additive Models in Ecology: An Introduction with *Mgc. PeerJ* **2019**, *7*, e6876. [[CrossRef](#)] [[PubMed](#)]
28. Rau, A.-L.; von Wehrden, H.; Abson, D.J. Temporal Dynamics of Ecosystem Services. *Ecol. Econ.* **2018**, *151*, 122–130. [[CrossRef](#)]
29. Li, W.; Wang, W.; Chen, J.; Zhang, Z. Assessing Effects of the Returning Farmland to Forest Program on Vegetation Cover Changes at Multiple Spatial Scales: The Case of Northwest Yunnan, China. *J. Environ. Manag.* **2022**, *304*, 114303. [[CrossRef](#)] [[PubMed](#)]
30. Li, F.; Zhou, W.; Shao, Z.; Zhou, X. Effects of Ecological Projects on Vegetation in the Three Gorges Area of Chongqing, China. *J. Mt. Sci.* **2022**, *19*, 121–135. [[CrossRef](#)]
31. Liu, S.; Liao, Q.; Xiao, M.; Zhao, D.; Huang, C. Spatial and Temporal Variations of Habitat Quality and Its Response of Landscape Dynamic in the Three Gorges Reservoir Area, China. *Int. J. Environ. Res. Public Health* **2022**, *19*, 3594. [[CrossRef](#)]
32. Li, C.; Qi, J.; Feng, Z.; Yin, R.; Guo, B.; Zhang, F.; Zou, S. Quantifying the Effect of Ecological Restoration on Soil Erosion in China's Loess Plateau Region: An Application of the MMF Approach. *Environ. Manag.* **2010**, *45*, 476–487. [[CrossRef](#)]
33. Vári, Á.; Kozma, Z.; Pataki, B.; Jolánkai, Z.; Kardos, M.; Decsi, B.; Pinke, Z.; Jolánkai, G.; Pásztor, L.; Condé, S.; et al. Disentangling the Ecosystem Service 'Flood Regulation': Mechanisms and Relevant Ecosystem Condition Characteristics. *Ambio* **2022**, 1–16. [[CrossRef](#)]
34. Battisti, L.; Corsini, F.; Gusmerotti, N.M.; Larcher, F. Management and Perception of Metropolitan Natura 2000 Sites: A Case Study of La Mandria Park (Turin, Italy). *Sustainability* **2019**, *11*, 6169. [[CrossRef](#)]
35. Battisti, L.; Pomatto, E.; Larcher, F. Assessment and Mapping Green Areas Ecosystem Services and Socio-Demographic Characteristics in Turin Neighborhoods (Italy). *Forests* **2019**, *11*, 25. [[CrossRef](#)]
36. Berglihn, E.C.; Gómez-Baggethun, E. Ecosystem Services from Urban Forests: The Case of Osloomarka, Norway. *Ecosyst. Serv.* **2021**, *51*, 101358. [[CrossRef](#)]
37. Jopke, C.; Kreyling, J.; Maes, J.; Koellner, T. Interactions among Ecosystem Services across Europe: Bagplots and Cumulative Correlation Coefficients Reveal Synergies, Trade-Offs, and Regional Patterns. *Ecol. Indic.* **2015**, *49*, 46–52. [[CrossRef](#)]
38. Pan, J.; Wei, S.; Li, Z. Spatiotemporal Pattern of Trade-Offs and Synergistic Relationships among Multiple Ecosystem Services in an Arid Inland River Basin in NW China. *Ecol. Indic.* **2020**, *114*, 106345. [[CrossRef](#)]
39. Vallet, A.; Locatelli, B.; Levrel, H.; Brenes Pérez, C.; Imbach, P.; Estrada Carmona, N.; Manlay, R.; Oszwald, J. Dynamics of Ecosystem Services during Forest Transitions in Reventazón, Costa Rica. *PLoS ONE* **2016**, *11*, e0158615. [[CrossRef](#)]
40. Feng, Q.; Zhao, W.; Fu, B.; Ding, J.; Wang, S. Ecosystem Service Trade-Offs and Their Influencing Factors: A Case Study in the Loess Plateau of China. *Sci. Total Environ.* **2017**, *607–608*, 1250–1263. [[CrossRef](#)]
41. Obiang Ndong, G.; Villerd, J.; Cousin, I.; Therond, O. Using a Multivariate Regression Tree to Analyze Trade-Offs between Ecosystem Services: Application to the Main Cropping Area in France. *Sci. Total Environ.* **2021**, *764*, 142815. [[CrossRef](#)]
42. Zhao, J.; Li, C. Investigating Ecosystem Service Trade-Offs/Synergies and Their Influencing Factors in the Yangtze River Delta Region, China. *Land* **2022**, *11*, 106. [[CrossRef](#)]
43. Xu, S.; Liu, Y.; Wang, X.; Zhang, G. Scale Effect on Spatial Patterns of Ecosystem Services and Associations among Them in Semi-Arid Area: A Case Study in Ningxia Hui Autonomous Region, China. *Sci. Total Environ.* **2017**, *598*, 297–306. [[CrossRef](#)] [[PubMed](#)]
44. Gong, J.; Liu, D.; Zhang, J.; Xie, Y.; Cao, E.; Li, H. Tradeoffs/Synergies of Multiple Ecosystem Services Based on Land Use Simulation in a Mountain-Basin Area, Western China. *Ecol. Indic.* **2019**, *99*, 283–293. [[CrossRef](#)]
45. Yang, Y.; Li, M.; Feng, X.; Yan, H.; Su, M.; Wu, M. Spatiotemporal Variation of Essential Ecosystem Services and Their Trade-off/Synergy along with Rapid Urbanization in the Lower Pearl River Basin, China. *Ecol. Indic.* **2021**, *133*, 108439. [[CrossRef](#)]
46. Peng, L.; Wang, X. What Is the Relationship between Ecosystem Services and Urbanization? A Case Study of the Mountainous Areas in Southwest China. *J. Mt. Sci.* **2019**, *16*, 2867–2881. [[CrossRef](#)]

47. Luo, R.; Yang, S.; Wang, Z.; Zhang, T.; Gao, P. Impact and Trade off Analysis of Land Use Change on Spatial Pattern of Ecosystem Services in Chishui River Basin. *Environ. Sci. Pollut. Res.* **2022**, *29*, 20234–20248. [[CrossRef](#)]
48. Chen, T.; Peng, L.; Wang, Q. Response and Multiscenario Simulation of Trade-Offs/Synergies among Ecosystem Services to the Grain to Green Program: A Case Study of the Chengdu-Chongqing Urban Agglomeration, China. *Environ. Sci. Pollut. Res.* **2022**, *29*, 33572–33586. [[CrossRef](#)]
49. Qiu, M.; Van de Voorde, T.; Li, T.; Yuan, C.; Yin, G. Spatiotemporal Variation of Agroecosystem Service Trade-Offs and Its Driving Factors across Different Climate Zones. *Ecol. Indic.* **2021**, *130*, 108154. [[CrossRef](#)]
50. Watson, S.C.L.; Newton, A.C.; Ridding, L.E.; Evans, P.M.; Brand, S.; McCracken, M.; Gosal, A.S.; Bullock, J.M. Does Agricultural Intensification Cause Tipping Points in Ecosystem Services? *Landsc. Ecol.* **2021**, *36*, 3473–3491. [[CrossRef](#)]
51. Xue, L.; Liang, H. Polynomial Spline Estimation for a Generalized Additive Coefficient Model. *Scand. J. Stat.* **2010**, *37*, 26–46. [[CrossRef](#)]
52. Wood, S.N. Fast Stable Direct Fitting and Smoothness Selection for Generalized Additive Models. *J. R. Stat. Soc. B* **2008**, *70*, 495–518. [[CrossRef](#)]
53. Wood, S.N.; Goude, Y.; Shaw, S. Generalized Additive Models for Large Data Sets. *J. R. Stat. Soc. C* **2015**, *64*, 139–155. [[CrossRef](#)]